Fast Electromagnetic Analysis of Multiscale Interconnect Networks using MultiAIM

Yongzhong Li, Damian Marek, and Piero Triverio
Edward S. Rogers Sr. Dept. of Electrical and Computer Engineering, University of Toronto, Toronto, ON, Canada
yongzhong.li@mail.utoronto.ca, damian.marek@mail.utoronto.ca, piero.triverio@utoronto.ca

***Abstract*—We propose a fast algorithm for the electromagnetic analysis of complex and multiscale interconnect networks in layered media. With a multigrid approach, we address the fundamental reason why the adaptive integral method (AIM) and pre-corrected FFT are inefficient for multiscale problems. Numerical tests with a preliminary implementation show that the proposed method is as accurate as AIM, but up to $16.8\times$ faster in the electromagnetic analysis of a complex interconnect network from a commercial integrated circuit, demonstrating the high potential of the proposed ideas.**

***Index Terms*—electromagnetic analysis, interconnect networks, multiscale, adaptive integral method, multigrid.**

I. Introduction

Full-wave electromagnetic (EM) analysis of electrical interconnects and electronic packages is direly needed to design, optimize, and validate next-generation electronic devices. However, the EM analysis of modern interconnects and packages is extremely time consuming, and often infeasible, due to their complexity. Furthermore, these structures are typically embedded in layered media and strongly multiscale, due to the simultaneous presence of large objects (e.g. ground planes) and tiny features (e.g. vias). Numerical methods that can accurately and efficiently simulate large, complex, and multiscale structures embedded in layered media are desperately needed.

A popular technique to solve Maxwell's equations for interconnect problems is the boundary element method (BEM). The BEM utilizes a surface mesh of conductive objects that can reduce the total number of unknowns considerably when compared to the finite element method or volumetric integral equation methods like PEEC. However, the BEM results in a dense system of equations. For large problems, this system must be solved iteratively with a fast algorithm to compute matrix-vector products. With layered media, the most popular acceleration method is the adaptive integral method (AIM) [1]–[3], or the closely-related pre-corrected Fast Fourier Transform (FFT) [2], [4]. Unfortunately, the AIM and pre-corrected FFT methods become very inefficient for multiscale structures, as they rely on a grid of *uniform* resolution to enable field propagation by FFT. Such a grid is intrinsically inefficient for such problems, since the mesh will unavoidably contain a mix of large and small triangles. For accuracy reasons, the largest mesh triangle will impose a relatively coarse resolution of the FFT grid. In turn, this will mean that many tiny triangles will fall in the near-region of each triangle, resulting in enormous integration costs to fill the near-region part of the BEM matrix [5].

Recently, we demonstrated that the efficiency of the AIM can be massively increased by: i) adapting the size of projection stencils to each triangle, ii) introducing a hierarchy of grids of different resolution as in multigrid methods [6], [7], iii) using the quasi-static Green's function in the near-region, and iv) exploiting voids and sparsity. The resulting technique, called MultiAIM [5], was previously developed for free space problems. In this paper, we generalize this approach to layered media and show preliminary results that confirm its high potential for accelerating the EM analysis of multiscale interconnects.

II. Formulation

We consider a set of conductive objects immersed in a layered medium and excited through lumped ports. We use the augmented electric field integral equation (AEFIE) to avoid low frequency breakdown [8] and the surface impedance boundary condition (SIBC) to model the skin effect [9].

In the AEFIE, the surface current density $\mathbf{J}_S$ and surface charge density ρ_S are both taken as unknowns. They are related by the electric field integral equation and by the continuity equation which, after discretization with the method of moments (MoM), read

$$\begin{bmatrix} jk_0\mathbf{L}^{(A)} + \eta_0^{-1}\mathbf{Z}_s & -\mathbf{D}^T\mathbf{L}^{(\phi)}\mathbf{B} \\ \mathbf{F}\mathbf{D} & jk_0\mathbf{I} + \mathbf{C} \end{bmatrix} \begin{bmatrix} \mathbf{J}_s \\ c_0\rho_s \end{bmatrix} = \begin{bmatrix} \mathbf{0} \\ \mathbf{I}_s \end{bmatrix}, \quad (1)$$

where k_0 is the wavenumber, η_0 is the wave impedance and c_0 is the phase velocity in free space. Dense matrices $\mathbf{L}^{(A)}$ and $\mathbf{L}^{(\phi)}$ are the vector and scalar parts of the electric field integral equation operator, which involve the multilayer Green's function (MGF). The SIBC is enforced by $\mathbf{Z}_s$. Vector $\mathbf{I}_s$ contains the excitation current injected at each port and matrix $\mathbf{C}$ provides coupling to the external circuit. Matrices $\mathbf{D}$, $\mathbf{F}$ and $\mathbf{B}$ are defined in [8].

In order to quickly solve (1) using an iterative method, matrix-vector products involving $\mathbf{L}^{(A)}$ and $\mathbf{L}^{(\phi)}$ must be computed rapidly. In the AIM, matrices $\mathbf{L}^{(A)}$ and $\mathbf{L}^{(\phi)}$ are split into near-region and far-region components as $\mathbf{L} = \mathbf{L}_N + \mathbf{L}_F$, where the near-region component must be computed using

This work was supported by Advanced Micro Devices, the Natural Sciences and Engineering Research Council of Canada and CMC Microsystems.

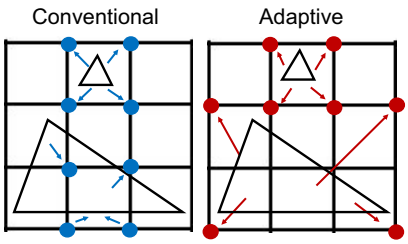

Fig. 1. The conventional stencils used in the AIM and the adaptive stencils used by the proposed method.

expensive numerical integrations involving the MGF. The far-region component is computed by introducing a regular grid and executing a series of steps that can be expressed using matrices as

$$\mathbf{L}_F = \mathbf{W}^{(0,1)}\mathbf{H}^{(1)}\mathbf{P}^{(1,0)} - \mathbf{L}_c. \tag{2}$$

In (2), $\mathbf{P}^{(1,0)}$ projects current and charge densities from the mesh triangles onto a set of nearby point sources, called a stencil. The point sources are chosen to produce the same fields (at sufficient distance). Then, $\mathbf{H}^{(1)}$, taking advantage of the 2D translational invariance of the MGF, quickly computes the fields produced by these sources on the same grid using 2D FFTs. Next, the fields are interpolated back from grid points to mesh triangles by $\mathbf{W}^{(0,1)}$. Since this process is inaccurate in the near region, a correction matrix $\mathbf{L}_c$ replaces the fields computed by FFT with the accurate ones obtained by integration. When a large frequency sweep is needed, these steps can be performed more efficiently using the extended AIM (AIMx) [10].

III. Proposed Method

For multiscale problems, the single uniform grid used by the AIM undermines its efficiency. The largest mesh triangle will impose a relatively large grid spacing, since each triangle must be contained in the projection stencil related to $\mathbf{P}^{(1,0)}$. Consequently, the near-region associated with each triangle will be large, and contain a high number of small triangles, leading to dense blocks in $\mathbf{L}_N$. Each entry in this block and in the related $\mathbf{L}_N$ must be computed by integrating the Green's function, which is very expensive, especially for layered substrates. If grid resolution is increased, accuracy will be compromised and FFTs will become very costly.

We can overcome these challenges in the following way. First, we adapt the size of projection stencils to the size of each triangle, as shown in Fig. 1. We devised an efficient procedure to scale the stencil of each triangle independently in each dimension, with minimal overhead for the necessary bookkeeping [5]. Adaptive stencils enable the use of an FFT grid of arbitrary resolution, no longer constrained by the largest triangle. Second, we introduce a hierarchy of L grids, as in multigrid algorithms [6], [7], with the goal of being able to control the resolution of the coarsest grid where FFTs are performed. The spacing of the grid at level $l+1$ is twice the spacing at level l, so we have $\Delta_{(l+1)} = 2\Delta_{(l)}$ for $l = 1, \ldots, L-1$. In our implementation, the number of grids L can be chosen independently along each direction, since interconnect layouts are usually very thin in the vertical dimension. With multiple grids, the far-region matrix $\mathbf{L}_F$ can be approximated as

$$\mathbf{L}_F \cong \mathbf{W}^{(0,1)}\left(\widetilde{\mathbf{H}}^{(1)} + \mathbf{H}_c^{(1)}\right)\mathbf{P}^{(1,0)} - \mathbf{L}_c\,, \tag{3}$$

where the new propagation matrix is defined recursively as

$$\widetilde{\mathbf{H}}^{(l)} = \begin{cases} \mathbf{W}^{(l,l+1)}\left(\widetilde{\mathbf{H}}^{(l+1)} + \mathbf{H}_c^{(l+1)}\right)\mathbf{P}^{(l+1,l)} & l = 1, ..., L-2 \\ \mathbf{W}^{(L-1,L)}\mathbf{H}^{(L)}\mathbf{P}^{(L,L-1)} & l = L-1 \end{cases}$$

and $l = 0$ denotes the triangular mesh. Matrix $\mathbf{P}^{(l+1,l)}$ projects sources from level l to level $l+1$. When level L is reached, matrix $\mathbf{H}^{(L)}$ propagates fields. For layered substrates, this matrix originates from the dyadic MGF, and comprises a vector and a scalar potential part

$$\mathbf{H}_{(A)} = \begin{vmatrix} \mathbf{H}_{xx}^{(L)} & 0 & \mathbf{H}_{xz}^{(L)} \\ 0 & \mathbf{H}_{yy}^{(L)} & \mathbf{H}_{yz}^{(L)} \\ \mathbf{H}_{zx}^{(L)} & \mathbf{H}_{zy}^{(L)} & \mathbf{H}_{zz}^{(L)} \end{vmatrix}, \mathbf{H}_{(\phi)} = \mathbf{H}_{(\phi)}^{(L)}. \tag{4}$$

The matrix-vector product of this propagator can be computed rapidly with 2D FFT in each xy plane. Finally, fields are interpolated back to lower level grids by $\mathbf{W}^{(l,l+1)}$, until the triangular mesh is reached. $\mathbf{H}_c^{(l)}$ is a correction matrix related to the singularity of the Green's function [5]. The use of multiple grids leads to an extremely efficient algorithm even for strongly multiscale layouts, capable of simultaneously resolving tiny details (with the finest grid) and propagating fields efficiently (with the coarsest grid). The required near region is so small that the quasi-static Green's function can be used to compute $\mathbf{L}_N$, for further gains [5]. Furthermore, we found that most grid points are not utilized, especially around voids in the layout. Such points can be detected with sparse matrix techniques and removed to compress all vectors and matrices [5]. The choice of grid resolution and number of levels L is fully automated for free space [5], and can be extended for layered medium.

IV. Numerical Results

A. Package microstrip benchmark

First, we tested the proposed method on a package microstrip benchmark [11], which features a single-ended microstrip with probe landing pads on both ends. We used a simplified substrate with the microstrip embedded in a dielectric layer with thickness 55.85 μm, and a layer of solder resist on top of thickness 33.55 μm. Conductors have conductivity $\sigma = 4.5 \times 10^7 S/m$. The structure was meshed with 82,566 triangles and 123,849 edges. The S-parameters were extracted from 100 MHz to 40 GHz and are shown in Fig. 2. The results from the proposed method are in excellent agreement with those from AIM and AIMx. From Table I, we see that the proposed method is 12.0× faster than AIM, reducing analysis time from 44.3 to 3.7 hours. The higher memory consumption is partly due to the preliminary implementation that is not yet optimized.

TABLE I
SIMULATION PARAMETERS, CPU TIME, AND MEMORY USAGE FOR THE TWO EXAMPLES IN SEC. IV-A AND IV-B

Testcase	Method	Levels	$\Delta_x^{(1)}, \Delta_y^{(1)}, \Delta_z^{(1)}$	CPU Time (h)				Memory (GB)
				Integration	Precorrection	Iterative Solution	Total	
Microstrip	**AIM**	1	$\lambda/81, \lambda/84, \lambda/151$	35.8	3.6	4.3	44.3	13
	AIMx	1	$\lambda/81, \lambda/84, \lambda/151$	0.7	0.1	6.5	7.4	13
	Proposed	3	$\lambda/349, \lambda/365, \lambda/226$	0.3	0.1	2.9	3.7	27
Network from real IC	**AIM**	1	$\lambda/1053, \lambda/1063, \lambda/1304$	131.9	8.8	12.4	168.5	106
	AIMx	1	$\lambda/1053, \lambda/1063, \lambda/1304$	6.6	0.9	12.5	20.7	106
	Proposed	3	$\lambda/4215, \lambda/4272, \lambda/1630$	3.1	1.0	4.6	10.0	157

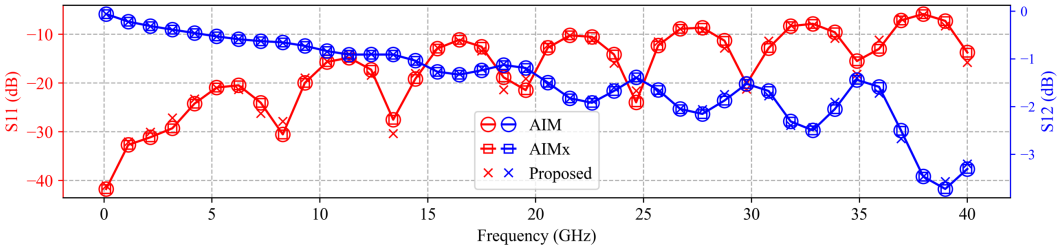

Fig. 2. Scattering parameters from 100 MHz to 40 GHz for the microstrip in Sec. IV-A.

B. High-speed interconnect from a real integrated circuit

The next example involves a portion of a high-speed communication bus from a commercial integrated circuit (courtesy of Advanced Micro Devices). The structure consists of an intricate network of wires and planes, with 65 distinct conductors of different size and shape. The mesh has 572,204 triangles and is strongly multiscale, with some triangles being 19 times smaller than others. Conductors are made of copper and placed in a 54.5 μm-thick dielectric layer with permittivity of 3.1. Excitation is applied through two lumped ports from 10 MHz to 50 GHz. In Fig. 3, the scattering parameters obtained from the three methods are reported, and are in very good agreement. Table I shows that the proposed approach significantly reduces integration, pre-correction and interative solution times compared to both the AIM and AIMx. Overall, the proposed method is 16.8× faster, reducing analysis time from 169 to 10 hours. Although from a preliminary implementation, these results demonstrate the high potential of the proposed approach for accelerating the analysis of real, complex and multiscale interconnect layouts from emerging 2.5D and 3D architectures.

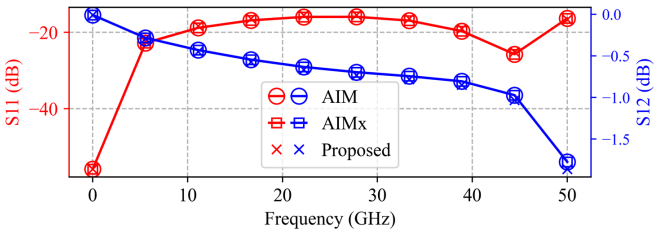

Fig. 3. Scattering parameters for the high-speed interconnect from a real IC.

REFERENCES

[1] E. Bleszynski, M. Bleszynski, and T. Jaroszewicz, "AIM: Adaptive integral method for solving large-scale electromagnetic scattering and radiation problems," *Radio Science*, vol. 31, no. 5, pp. 1225–1251, Sep. 1996.

[2] V. Okhmatovski, M. Yuan, I. Jeffrey, and R. Phelps, "A three-dimensional precorrected FFT algorithm for fast method of moments solutions of the mixed-potential integral equation in layered media," *IEEE Trans. Microw. Theory Techn.*, vol. 57, no. 12, pp. 3505–3517, Dec. 2009.

[3] K. Yang and A. E. Yilmaz, "A three-dimensional adaptive integral method for scattering from structures embedded in layered media," *IEEE Trans. Geosci. Remote Sens.*, vol. 50, no. 4, pp. 1130–1139, Apr. 2012.

[4] J. R. Phillips and J. K. White, "A precorrected-FFT method for electrostatic analysis of complicated 3-D structures," *IEEE J. Technol. Comput. Aided Design*, vol. 16, no. 10, pp. 1059–1072, 1997.

[5] Y. Li, D. Marek, and P. Triverio, "MultiAIM: Fast electromagnetic analysis of multiscale structures using boundary element methods," TechRxiv, 2023, doi: 10.36227/techrxiv.23560692.v1.

[6] A. Brandt, "Multilevel computations of integral transforms and particle interactions with oscillatory kernels," *Comput. Phys. Commun.*, vol. 65, no. 1-3, pp. 24–38, 1991.

[7] K. Yang, F. Wei, and A. E. Yilmaz, "Truncated multigrid versus precorrected FFT/AIM for bioelectromagnetics: When is O(N) better than O(NlogN)?" in *CEM'11 Comput. Electromagn. Int. Workshop*. IEEE, Aug. 2011, pp. 153–158.

[8] Z. G. Qian and W. C. Chew, "Fast full-wave surface integral equation solver for multiscale structure modeling," *IEEE Trans. Antennas Propag.*, vol. 57, no. 11, pp. 3594–3601, 2009.

[9] S. Yuferev and N. Ida, *Surface Impedance Boundary Conditions*. CRC Press, 2009.

[10] S. Sharma and P. Triverio, "AIMx: An extended adaptive integral method for the fast electromagnetic modeling of complex structures," *IEEE Trans. Antennas Propag.*, vol. 69, no. 12, pp. 8603–8617, 2021.

[11] "Packaging Benchmark Suite," 2021. [Online]. Available: https://packaging-benchmarks.org/